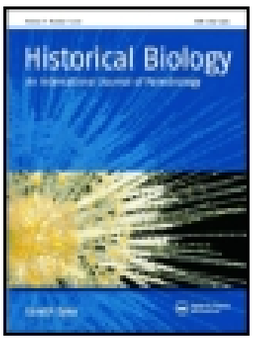

Historical Biology

An International Journal of Paleobiology

ISSN: 0891-2963 (Print) 1029-2381 (Online) Journal homepage: http://www.tandfonline.com/loi/ghbi20

Femoral osteopathy in *Gigantspinosaurus sichuanensis* (Dinosauria: Stegosauria) from the Late Jurassic of Sichuan Basin, Southwestern China

Bao-Qiao Hao, Yong Ye, Susannah C R. Maidment, Sergio Bertazzo, Guang-Zhao Peng & Hai-Lu You

To cite this article: Bao-Qiao Hao, Yong Ye, Susannah C R. Maidment, Sergio Bertazzo, Guang-Zhao Peng & Hai-Lu You (2018): Femoral osteopathy in *Gigantspinosaurus sichuanensis* (Dinosauria: Stegosauria) from the Late Jurassic of Sichuan Basin, Southwestern China, Historical Biology, DOI: 10.1080/08912963.2018.1561673

To link to this article: https://doi.org/10.1080/08912963.2018.1561673

Published online: 31 Dec 2018.

HISTORICAL BIOLOGY
https://doi.org/10.1080/08912963.2018.1561673

Taylor & Francis
Taylor & Francis Group

ARTICLE

Femoral osteopathy in *Gigantspinosaurus sichuanensis* (Dinosauria: Stegosauria) from the Late Jurassic of Sichuan Basin, Southwestern China

Bao-Qiao Hao[a,b], Yong Ye[a], Susannah C R. Maidment[c], Sergio Bertazzo[d], Guang-Zhao Peng[a] and Hai-Lu You[e,f]

[a]Zigong Dinosaur Museum, Zigong, China; [b]State Key Laboratory of Palaeobiology and Stratigraphy, Nanjing Institute of Geology and Palaeontology, Chinese Academy of Sciences, Nanjing, China; [c]Department of Earth Sciences, Natural History Museum, London, UK; [d]Department of Medical Physics and Biomedical Engineering, University College London, London, UK; [e]Key Laboratory of Vertebrate Evolution and Human Origins, Institute of Vertebrate Paleontology and Paleoanthropology, Chinese Academy of Sciences, Beijing, China; [f]CAS Center for Excellence in Life and Paleoenvironment, Beijing, China

ABSTRACT

We report a case of a specific osteopathy in the stegosaurian dinosaur *Gigantspinosaurus sichuanensis* from the Late Jurassic of Zigong City, China. The *G. sichuanensis* skeleton is very complete. The left femur has obvious pathological characteristics based on morphological observations. CT scans and energy spectrum data indicate the presence of multiple cystic-like low density areas internal to the pathological area, which are present in the form of multiple cystic low-density shadows in the CT data. This contrasts with the 'normal' area, which does not possess these characteristics. After comparing the specimen with the pathologic scapula of *Yangchuanosaurus hepingensis* (Dinosauria: Theropoda) also found in Zigong, we consider that the pathology in the left femur of *G. sichuanensis* was probably caused by a bone tumor. This is the first analysis with the aid of energy spectrum CT scanning of bone disease in fossils. This study increases the known information about paleopathology of stegosaurian dinosaurs and enriches the pathological knowledge of dinosaurs in general.

ARTICLE HISTORY
Received 6 October 2018
Accepted 18 December 2018

KEYWORDS
Stegosauria; bone pathology; Sichuan Basin; energy spectrum CT

Stegosauria is a clade of dinosaurs characterized by the possession of two parasagittal rows of dermal armour extending from the neck to the end of the tail. Although progress has been made concerning our understanding of the morphology and phylogeny of stegosaurs (Dong et al. 1982; Zhou et al., 1984; Maidment and Wei 2006; Jia et al. 2007; Maidment et al., 2008; Maidment 2010; Maidment et al. 2015; Raven and Maidment 2017), the record of illness or injury in stegosaurs has been reported less frequently (Carpenter et al. 2005). *Gigantspinosaurus sichuanensis* is a stegosaur found in the Upper Shaximiao Formation (Late Jurassic) of Zigong, Sichuan Province, People's Republic of China. Its holotype specimen is a very well-preserved skeleton that not only preserved the world's first stegosaur skin impression (Ouyang et al. 1998), but also for the first time the parascapular spines were found associated with the scapulocoracoid (Ouyang 1991). The left and right femora of the skeleton are preserved intact, and there is a big difference between the two in appearance. The left femur exhibits obvious pathological features, which provides good material for pathological research.

There has been much research on dinosaur bone pathology, e.g. Molnar (2001); Rega (2012); Butler et al. (2013); Rothschild et al. (1999), Rothschild (2010), 2012); Rothschild and Tanke (2005); Rothschild and Panza (2005); Anné et al. (0, 2015)); Farke and O'Connor (2007);. Hanna (2002); Hone and Tanke (2015); Lü et al. (2007); Arbour and Currie (2011); Dumbravă et al. (2016); García et al. (2016); Barbosa et al. (2016); Hedrick et al. (2016); Gonzalez et al. (2017); Witzmann et al. (2008, 2014)); Xing et al. (2009), Xing et al. (2018)). Initial research was generally limited to morphological descriptions, not to sectional analysis (e.g. Chinsamy-Turan 2005; Lü, 2007), and thus these findings were less convincing. Some scholars used CT scans and bone histology to explain pathological phenomena in dinosaurs and analyzed the healing of fractures and the causes of bone diseases (e.g. Straight et al. 2009; Hedrick et al. 2016). The main feature of CT scans is the observation of the internal structure of fossils, and there is no damage to the fossil itself. In order to achieve the high resolution necessary to elucidate detail and small structures within fossils, micro-CT scanners have been used (Morgan et al. 2009). However, micro-CT scanners are generally too small for large material such as the femora of stegosaurian dinosaurs, which are typically between 80 and 120 cm in length (SCRM pers. obs). Medical or veterinary CT scanners, which are larger, may lack the resolution to elucidate small-scale features in fossils as their slice thickness is limited to around 1–2 mm (but see Sampson and Witmer 2007, Witmer and Ridgely 2008a, 2008b for some successful examples). Sutton (2008) has provided a detailed review of CT-scanning techniques applied to palaeontological research. In this paper, medical energy spectrum CT scanning technology of Gemstone Spectrum Imaging (GSI) has been used. In traditional CT, evaluate material only material density, expressed with CT value. However, two kinds of different materials, such as a bottle of salt and a bottle of sugar water, the same CT

CONTACT Bao-Qiao Hao Haobaoqiao1984@163.com Zigong Dinosaur Museum, Zigong 643013, China

Published online 31 Dec 2018

value can be measured, cannot show the differences between the two components. Energy spectrum CT is described with CT value beyond the purely physical limitations, use of different single energy X beam through the specific objects, its CT value with the increase or decrease of X-ray energy changing regularity, formed a characteristic spectral lines, the line is only related to the nature of the material itself, and the spectral lines of different materials, began to detect the exact material, improve the level of differential diagnosis (Murali et al. 2011).

Material and methods

The complete, articulated skeleton was excavated from the Upper Shaximiao Formation of Pengtang in Yinhe Village, Zhongquan Town, Zigong City, Sichuan Province in 1985. The Upper Shaximiao Formation has yielded a diversity of fossils known as the '*Mamenchisaurus* Fauna', and includes the other stegosaurs *Tuojiangosaurus multispinus*, and *Chungkingosaurus jiangbeiensis* (Dong et al. 1983; Peng et al. 2005; Maidment and Wei 2006). Recent isotopic dating of the Lower Shaximiao Formation, which underlies the Upper Shaximiao Formation, places it at 159 ± 2 Ma (Wang et al. 2018), suggesting that the Upper Shaximiao Formation is likely to be Kimmeridgian to Tithonian in age. This is consistent with other stegosaur-bearing terrestrial faunas, such as the Morrison Formation of the USA and the Tendaguru Formation of Tanzania.

Gigantspinosaurus sichuanensis (ZDM 0019), an almost complete skeleton, including both mandibles, eight cervical vertebrae, 16 dorsal vertebrae, four sacral vertebrae, some anterior caudal vertebrae, parts of the appendicular skeleton, parts of osteoderms, and a pair parascapular spines (the right one with a small skin impression). The skeleton represents a single individual, as it was found in articulation (Hao et al. 2018).

Institutional abbreviations: NHMUK; Natural History Museum, London, UK; ZDM, Zigong Dinosaur Museum, Sichuan, China (Figure 1).

In this study, medical energy spectrum CT (GSI) scanning, three-dimensional reconstruction and data analysis techniques were used on the two femora of *Gigantspinosaurus sichuanensis*, focusing on the pathologic area. Energy spectrum CT can use two basic substances to draw the energy spectrum curve of the measured substance, and then compare it with the energy spectrum curve of a known substance to understand the composition of the substance. Calcium and water were used as the base substances in this case, which provides direct evidence for the analysis of fossil lesions. The energy spectrum CT machine is a GE Revolution CT scanner from the Department of Radiology of Zigong First People's Hospital, Sichuan Province, China.

Initially, the whole femora were scanned, using axis sweep. The relevant parameters are KeV140, 600 mAs, the bulb speed 1 s, and the slice thickness 0.625 mm. Subsequently, energy spectrum scanning was performed on the pathologic area and the 'normal' area. The relevant parameters are 80–140 KeV switching, 485 mAs, pitch 0.516:1, bulb speed 0.5 s, slice thickness 0.625 mm. Finally, the analysis of the energy spectrum of the energy-based material and the drawing of the energy spectrum of the relevant region were carried out.

We performed 3D imaging, conventional CT and energy spectrum CT scans on the left and right femora. Energy spectrum CT removes the hardened artefact interference of the 140 kpV mode of hybrid energy and uses the instantaneous switching of high and low dual energy (80 kVp and 140 kVp) in a single tube to generate fully matched dual-energy data in space-time.

Specimen description

The left and right femora are both well-preserved. The femora are slightly deformed at the ventral end of the right side, but the other parts of the femora have not been deformed by burial. The right femur is straight in lateral view, the bone surface is smooth, the transverse section of the shaft is oblate, and it is 67 cm long. Proximally, the femoral head projects medially, the greater trochanter is present as an anteroposterior expansion on the lateral surface, and the lesser trochanter is not clearly defined. The fourth trochanter is weakly developed, and located at midlength of the femoral shaft. Distally, the medial condyle is slightly larger than the lateral condyle. There is a prominent groove on the lateral side of the lateral condyle for attachment of tendons, and the posterior intercondylar groove is obvious. In all respects it is similar to the femora of other stegosaurs, e.g. *Stegosaurus* (NHMUK PV R36730; Maidment et al. 2015).

The left femur showed obvious abnormalities relative to the right, with the shaft thickened. Under normal circumstances, both sides should be basically symmetrical. Therefore, it is presumed that there is a pathology, or lesion, on the left femur.

Pathological discussions

Morphological pathological analysis

The left femur is thicker than the right femur at mid shaft, and the middle and lower part of the shaft is swollen, resulting in the fourth trochanter not being visible. The bulge is longitudinal ridge-like structure, with a smooth surface. The bone appears to be bent along its proximodistal axis. This is an obvious fracture. According to whether bone tissue before fracture is normal, Bone fractures can be divided into traumatic fractures and pathological fractures, which depend on whether the bone tissue was normal or pathologic before the fracture occurred. In traumatic fractures, the bone cortex is broken and discontinuous (Qin 2004). The bone cortex is continuous on the left femur, especially the medial posterior view (left side of Figure 2(c)) of *Gigantspinosaurus* and thus we conclude that the pathology is probably a pathological fracture.

CT image analysis

Images of the transverse view, the coronal view, and the sagittal view were used to perform the pathological analysis.

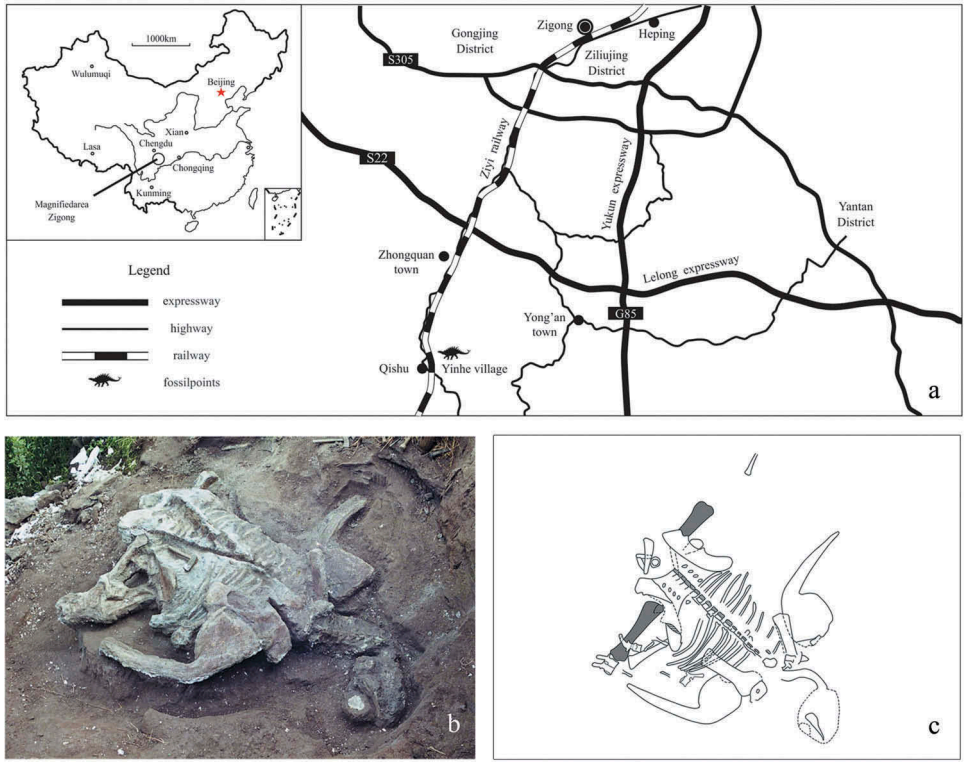

Figure 1. Photograph and line drawing of *Gigantspinosaurus sichuanensis* during its excavation.

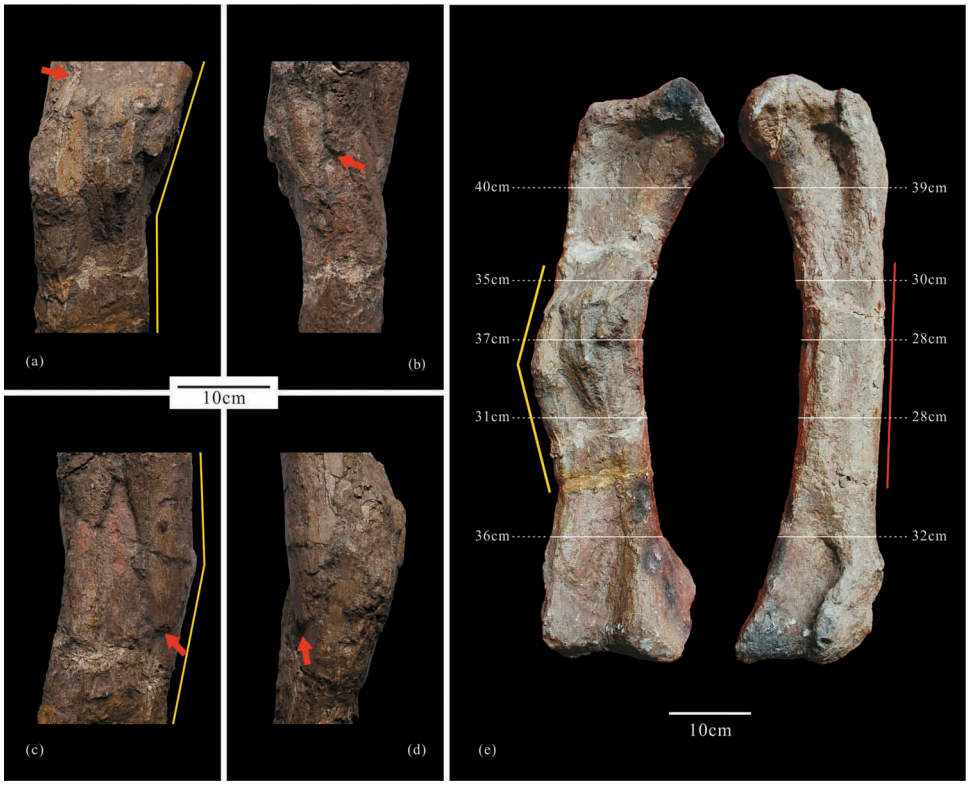

Figure 2. External morphology of the femur preserved left and right femurs and omnidirectional visual image of the left femur lesion area. (a) rear view of the lesion; (b) medial view of the lesion; (c) front view of the lesion; (d) lateral view of the lesion; (e) rear view of the left and right femurs, where the numbers indicate the circumference here, scale bar = cm. The yellow line shows bone line bending, suggesting a bone fracture. The red line is the normal force line. Red arrows indicate that the bones were distorted or misaligned.

Right femur

The shape of the shaft is regular, the bone cortex and the marrow cavity are clearly displayed, and the boundary is obvious and continuous. A break that occurred during excavation was pasted with glue, showing up as a black line on the CT scan. When scanning the middle part of the femur with energy spectrum CT, several oval anomaly areas of different sizes could be observed.

Left femur

The shape of the shaft is irregular, the boundary between the bone cortex and the marrow cavity is not clear, and the marrow cavity is indistinct compared with the right one. In the expanded bone cortex and the marrow cavity, many circular or elliptical multiple cystic-like low-density areas of different sizes are visible, and the boundary of the cystic-like low-density areas is clear and separated from each other.

According to the energy spectrum CT images of the whole bone and the fractured area, the boundary between the bone marrow and the bone cortex is obvious in the right femur, being smooth and continuous. The circumference of the left femur was significantly thicker than the right one. The bone cortex is morphologically different and the lateral cortex is continuous. The oval cyst-like structures are concentrated on one side of the left femur, and there are obvious cystic-like structures, with clear boundaries and a thinner cortex. This structure is called a cystic lesion in modern medicine (Baker 1970; Dios et al. 1992) and is a direct manifestation of bone disease. Combined with the CT images, the lesion area has multiple cystic low-density shadows with reduced density, and a similar shaded area is also found in the right femur. This pathological phenomenon may occur in bone diseases such as fibrous dysplasia of bone, multiple bone cysts and aneurysmal bone cysts (Riminucci et al. 1997; Hart et al. 2007; Rothschild et al. 2018). Based on current evidence, the structure appears to be a bone tumour, but it is somewhat difficult to specify which one, so it is only classified as bone tumour for the time being.

The left femur is distorted so that the proximal and distal ends are offset from one another in the bone lesion area. It is speculated that the bone structure changed due to bone disease, the strength was reduced, and a fracture occurred as a result (Figure 3).

Energy spectrum data analysis

The energy spectrum data is formed by the same material under different X-rays of different single-energy electrons, which reflects the attenuation characteristics (and attenuation coefficient) of the substance. The attenuation coefficient of each substance is specific, so it can be analyzed. The energy spectrum CT can be used to display the material of the specimen in certain proportions, such as the calcium to water ratio. The energy spectrum curve is drawn from normal

Figure 3. CT images of the femoral energy spectrum. (a) 3D rear view of the left and right femora; (b) CT images of the left and right femora, red arrows indicating the boundary between the cortical and medullary cavities; (c) sagittal CT images of the left and right femora; (d) CT images of the transverse axis of the lesions, red indicates lesioned bone and yellow indicates healthy bone; (e) Coronal CT image of the lesion, the enlarged part shows more obvious cystic structure, the boundary between it is clear; (f) Coronal CT image of the lesion.

areas of the left and right femora (Figure 4). It can be seen in Figure 4 that the energy spectrum curve measured as shown in Curve 1 coincides with Curve 2, and the energy spectrum curves measured by Curve 3 and Curve 4 coincide, suggesting a high possibility of the same substance. According to the images, it can be seen that Curve 1 and Curve 2 are bone marrow cavities, and Curve 3 and Curve 4 are bone cortex.

Taking the point from the left femur lesion area No.5, the energy spectrum curve was drawn. It was found that the curve is clearly different from the normal marrow cavity and the cortex. It is considered that the lesion is dissimilar to the marrow cavity and the cortex, and is not a normal bone structure.

In addition, a suspicious lesion No.6 was found in the bone marrow cavity of the normal right femur adjacent to the cortex, showing a shadow similar to the lesion on the left femur. The energy spectrum curve was drawn and analyzed. The curves and the spectrum of the right femur lesions are consistently parallel and show a very good consistency to the left femur. Therefore, there may also be some lesions in the right femur, and it is further inferred that the bone disease is multifocal, resulting in a high degree of consistency in the energy spectrum curve, but not yet to the extent that the shape of the bone is changed or the bone has fractured.

Analysis of the energy spectrum curve data shows that despite fossilization, there are still great differences in the composition of the bone marrow cavity and the cortex. The performance of the energy spectrum curve and the base material in the left femur lesion area analysis result are distinctively different from the bone marrow cavity and the cortex. The homology was shown in the same regions of the left and right femurs, such as bone cortex, bone marrow

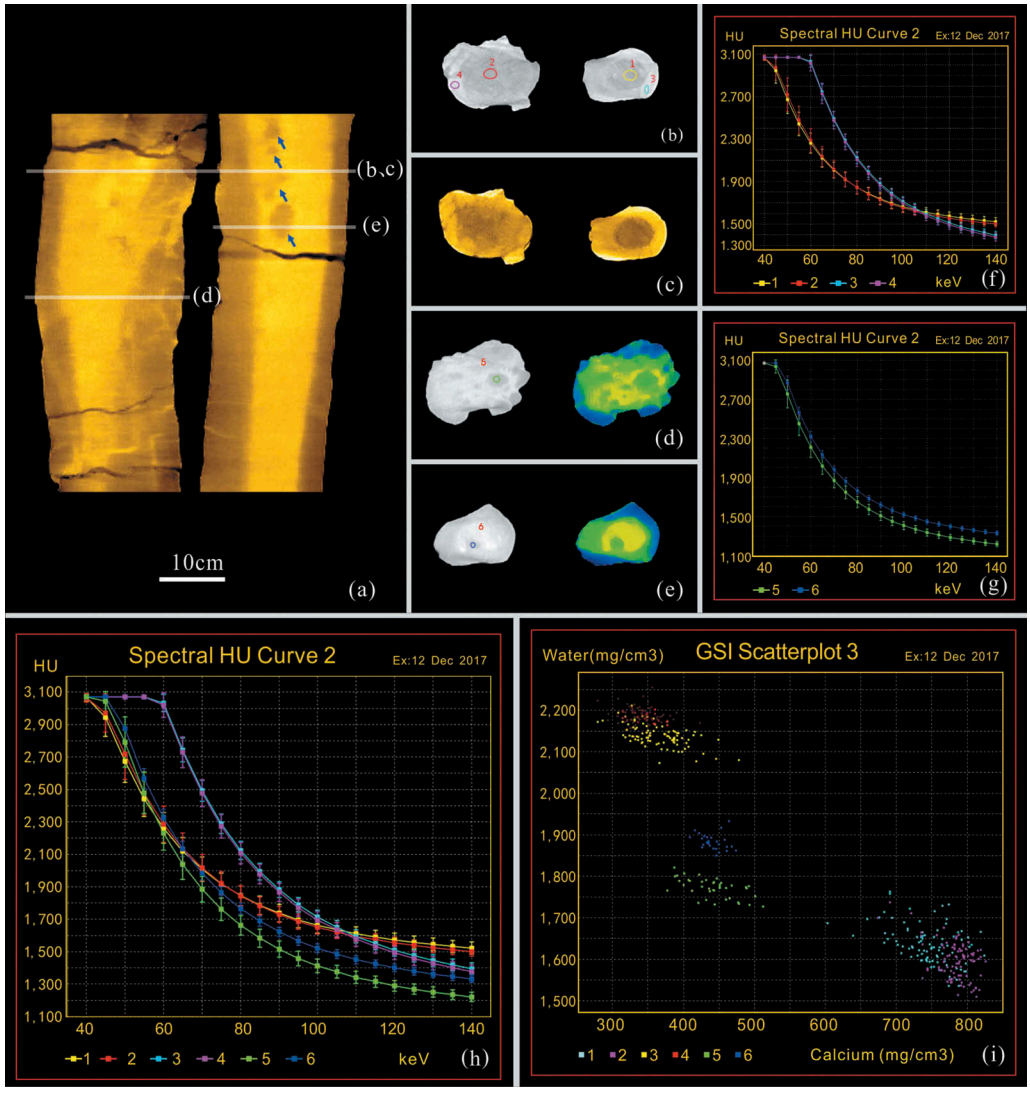

Figure 4. Energy spectrum data analysis of the femurs. (a) Coronal colour image of the left and right femoral lesions, blue arrow indicating the shadow of the suspected lesion on the right femur; (b) CT image of the transverse view of the normal region of the left and right femurs, numbers showing the picking points from different regions to draw the energy spectrum curve; (c) CT colour image of the transverse view of normal area of the left and right femur; (d) CT image of the transverse view of the left femur lesion area, drawing the point of the lesion shadow area; (e) CT image of the transverse view of the suspected lesion area of the right femur, drawing the point of the shadow area of the suspected lesion; (f) The energy spectrum curve, taking the points from the normal area. The energy spectrum curve coincides, that 1 and 2 are the marrow cavity, 3 and 4 are the cortex; (g) The right femur suspicious area and the left femur lesion area draw a highly consistent and parallel energy spectrum curve, showing a very good homological relationship; (h) The energy spectrum curve of the lesion area is different from the normal marrow cavity and cortex, showing that it is not normal bone structure; (i) Using calcium-based materials to compare several regions, similar regions have obvious homology, while different regions have clear non-homology.

cavity, and shadow area. Therefore, it shows that deposition has little impact and the difference is only due to the difference of original components. These are therefore considered to not be normal bone structures. Observing the energy spectrum CT, some similar shadows with the lesion area were also found on the right side of the normal femur. The results were consistent with the height of the energy spectrum curve of the left femur lesion area, showing very good consistency. It is speculated that this stegosaur had a bone disease, and it was not restricted to one bone.

Comparative analysis

When the bone fractures, the outline of it will be expanded. For example, the fracture of the scapula in *Yangchuanosaurus hepingensis* (ZDM 0024): the fractured bone is significantly larger than the normal one. When the traumatic fracture is healing, most of the bone cortex is not smooth, and clear disordered trabeculae of a bone callus is formed (Figure 5). In the CT scan, the marrow will show obvious discontinuity, the stress line of the scapula will be curved, and the bony callus attached to the bone cortex can be seen in some areas.

These features are not visible in the left femur of *Gigantspinosaurus*. In outline, the expansion takes the form of a longitudinal ridge, a non-bony callus structure. There is a smooth surface on the bone: no exostosis or osteoporosis structure is visible. According to the CT results, the lesions were concentrated on the left femur, and there were obvious cystic structures. The boundary was clear and the bones were separated, while the lateral cortices were continuous. In addition, a similar but less developed structure was found in the normal right femur. The data analysis shows that the composition was also the same. We, therefore, conclude that the pathological case on the femur of *Gigantspinosaurus sichuanensis* was not caused by a traumatic fracture, but by a bone disease. The bone disease itself caused the structural change of the bone, reducing its strength and the abnormal concentration of stress of the bone, resulting in a fracture. This is manifested in a distortion of the left femur.

The explanation of the pathology of *Gigantspinosaurus sichuanensis* may also include: the pathology may be adjacent to the fracture; the pathology is an infection occurring secondary to the fracture; a comminuted fracture. However, based on the above evidence, the article is more inclined to pathological fracture. Subsequent, more in-depth and reliable conclusions depend on better modern research methods, such as histology.

Conclusions

Paleopathology uses modern medical methods to provide a physiological explanation for pathologies in ancient extinct animals. Combined with advanced medical energy spectrum CT, we found multiple cystic structures on the femur of the stegosaur *Gigantspinosaurus*. Multiple cystic low density shadows could be seen in the pathologic area.

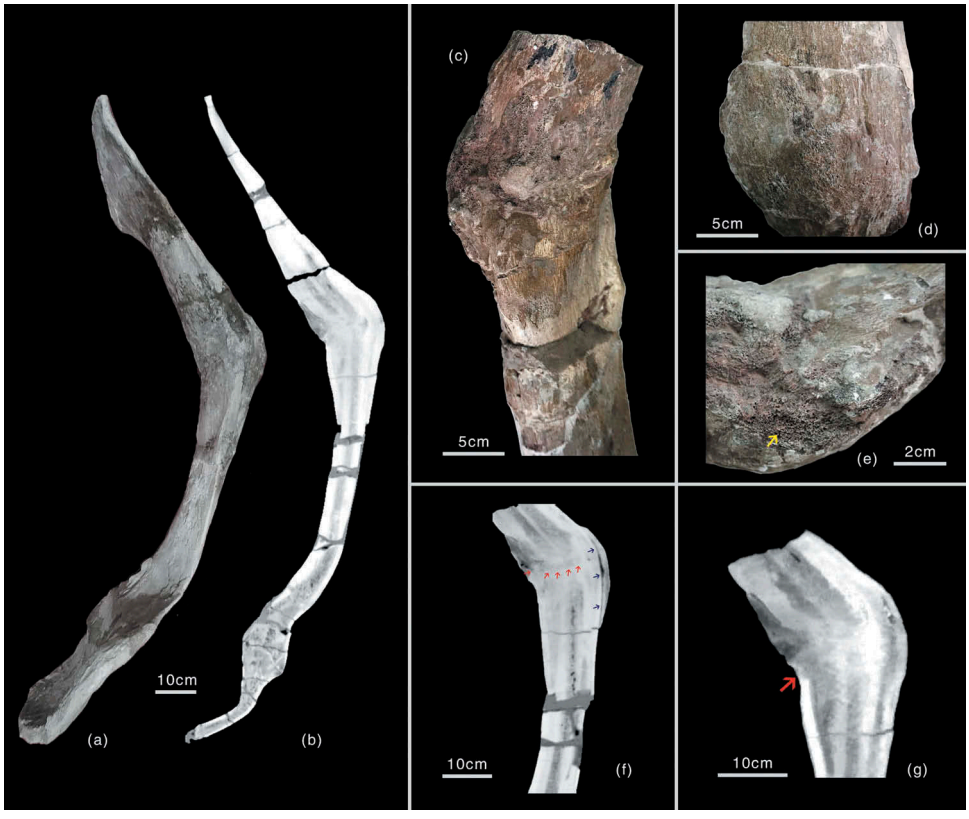

Figure 5. Analysis of the fracture of the left scapula of *Yangchuanosaurus hepingensis*. (a) morphological image of the left scapula of *Y. hepingensis* in medial view; (b) CT image of the left scapula of *Y. hepingensis*; (d) the expanded area of the fracture; (e) detailed image of the fracture, visible honeycomb structure; (f) CT image of the fracture area, red arrow indicates the fracture line, the yellow arrow shows the trace line of the poroma attached to the bone cortex; (g) detailed CT image of the fracture area.

In the normal shaped right femur, there were areas of suspected lesions on the image and energy spectrum data. It is speculated that the bone tumor is a non-single bone tumor. This discovery enriched the paleopathology of dinosaurs in China and enriches our knowledge of pathologies experienced by dinosaurs. Advanced medical instruments allow us to get a more reasonable explanation from images and data. According to the energy spectrum curve and the ratio of the base materials, we conclude that this stegosaur had a multifocal bone disease, which produced a series of differences in external morphology. This is the first analysis of the energy spectrum of bone disease in fossils, and contributes to our understanding of the living conditions of the extinct creatures hundreds of millions of years ago.

Acknowledgments

We would like to acknowledge the assistance and help of the following people in the production of this research: Mr FENG Hao and Mr ZHAO Zhi-Qiang from Zigong First People's Hospital, GE CT training specialist Mr WAN Du-xing provided relevant images and data support. Mr HUANG Da-xi, Mr OUYANG Hui and Mr JIANG Shan provided valuable field geological materials. Ms LING Man, Ms LUO Shu drew the illustrations.

Disclosure statement

No potential conflict of interest was reported by the authors.

Funding

This research was funded by the State Key Laboratory of Palaeobiology and Stratigraphy (Nanjing Institute of Geology and Palaeontology, Chinese Academy of Sciences) (No. 183109), and Sichuan Province Land and Resources Department Project 'Dinosaur fossil resources protection and development and utilization model in Sichuan Basin' (No. KJ-2017-11).

ORCID

Hai-Lu You http://orcid.org/0000-0003-2203-6461

References

Anné J, Garwood RJ, Lowe T, Withers PJ, Manning PL. 2015. Interpreting pathologies in extant and extinct archosaurs using micro-CT. Peer J. 3:e1130.

Anné J, Hedric BP, Schein JP. 2016. First diagnosis of septic arthritis in a dinosaur. Roy Soc Open Sci. 3:160222.

Arbour VM, Currie PJ. 2011. Tail and pelvis pathologies of ankylosaurian dinosaurs. Hist Biol. 23:375–390.

Baker DM. 1970. Benign unicameral bone cyst. A study of forty-five cases with long-term follow up. Clin Orthop Relat Res. 71:140–151.

Barbosa FHS, Pereira PVLG, Bergqvist LP, Rothschild BM. 2016. Multiple neoplasms in a single dinosaur from the Upper Cretaceous of Brazil. Cretac Res. 62:13–17.

Butler R, Yates A, Rauhut O, Foth C. 2013. A pathological tail in a basal sauropodomorph dinosaur from South Africa: evidence of traumatic amputation? J Vert Paleont. 33:224–228.

Carpenter K, Sanders F, McWhinney L, Wood L. 2005. Evidence for predator-prey relationships: examples for Allosaurus and Stegosaurus. In: Kenneth C, editor. The carnivorous dinosaurs. Bloomington (IN): Indiana University Press; p. 325–350.

Chinsamy-Turan A. 2005. The microstructure of dinosaur bone: deciphering biology with fine-scale techniques. Baltimore (Maryland): Johns Hopkins University Press; p. 1–216.

Dios AM, Bond JR, Shives TC, McLeod RA, Unni KK. 1992. Aneurysmal bone cyst. A clinicopathologic study of 238 cases. Cancer. 69:2921–2931.

Dong ZM, Tang ZL, Zhou SW. 1982. Note on the new Mid-Jurassic Stegosaurian from Sichuan Basin, China. Vert Palasiat. 20:83–86. In Chinese.

Dong ZM, Zhou SW, Zhang YH. 1983. Dinosaurs from the Jurassic of Sichuan. Palaeont Sin. 162:1–136. In Chinese.

Dumbravă MD, Rothschild BM, Csiki-Sava Z, Andrei A, Solomon AA, Codrea VA. 2016. A dinosauran facial deformity and the first occurrence of ameloblastoma in the fossil record. Sci Rep. 6:29271.

Farke AA, O'Connor PM. 2007. Pathology in *Majungasaurus crenatissimus* (Theropoda: Abelisauridae) from the Late Cretaceous of Madagascar. J Vertebr Paleont. 27:180–184.

García RA, Cerda IA, Heller M, Rothschild BM, Zurriaguz V. 2016. The first evidence of osteomyelitis in a sauropod dinosaur. Lethaia. 50:227–236.

Gonzalez R, Gallina PA, Cerda IA. 2017. Multiple paleopathologies in the dinosaur *Bonitasaura salgadoi* (Sauropoda: Titanosauria) from the Upper Cretaceous of Patagonia, Argentina. Cretac Res. 79:159–170.

Hanna RR. 2002. Multiple injury and infection in a sub adult theropod dinosaur *Allosaurus fragilis* with comparisons to allosaur pathology in the Cleveland-Lloyd Dinosaur Quarry Collection. J Vert Paleont. 22:76–90.

Hao BQ, Zhang QN, Peng GZ, Ye Y, You HL. 2018. Redescription of *Gigantspinosaurus sichuanensis* (Dinosauria, Stegosauria) from the Late Jurassic of Sichuan, Southwestern China. Acta Geol Sin (English Edition). 92:431–441.

Hart ES, Kelly MH, Brillante B, Chen CC, Ziran N, Lee JS, Feuilla P, Leet AI, Kushner H, Robey PG, et al. 2007. Onset, progression, and plateau of skeletal lesions in fibrous dysplasia and the relationship to functional outcome. J Bone Min Res. 22:1468–1474.

Hedrick BP, Gao C, Tumarkin-Deratzian AR, Shen C, Holloway JL, Zhang F, Hankenson KD, Liu S, Anné J, Dodson P. 2016. An injured *Psittacosaurus* (Dinosauria: Ceratopsia) from the Yixian Formation (Liaoning, China): implications for Psittacosaurus biology. Anat Rec. 299:897–906.

Hone DWE, Tanke DH. 2015. Pre- and postmortem tyrannosaurid bite marks on the remains of *Daspletosaurus* (Tyrannosaurinae: Theropoda) from Dinosaur Provincial Park, Alberta, Canada. PeerJ. 3:e885.

Jia C, Forster CA, Xu X, Clark J. 2007. The first stegosaur (Dinosauria, Ornithischia) from the Upper Jurassic Shishugou Formation of Xinjiang, China. Acta Geol Sin (English Edition). 81:351–356.

Lü JC, Kobayashi Y, Lee YN, Ji Q. 2007. A new *Psittacosaurus* (Dinosauria: Ceratopsia) specimen from the Yixian Formation of western Liaoning, China: the first pathological psittacosaurid. Cretac Res. 28:272–276.

Maidment SCR. 2010. Stegosauria: a historical review of the body fossil record and phylogenetic relationships. Swiss J Geosci. 103:199–210.

Maidment SCR, Brassey C, Barrett PM. 2015. The postcranial skeleton of an exceptionally complete individual of the plated dinosaur *Stegosaurus stenops* (Dinosauria: Thyreophora) from the Upper Jurassic Morrison Formation of Wyoming, U.S.A. PLoS One. 10: e0138352.

Maidment SCR, Norman DB. 2008. Systematics and phylogeny of Stegosauria (Dinosauria: Ornithischia). J Syst Palaeontol. 6:367–407.

Maidment SCR, Wei GB. 2006. A review of Late Jurassic stegosaurs (Dinosauria, Stegosauria) from the People's Republic of China. Geol Mag. 143:621–634.

Molnar RE. 2001. Theropod paleopathology: a literature survey. In: Tanke DH, Carpenter K, editors. Mesozoic vertebrate life. Bloomington (IN): Indiana University Press; p. 337–363.

Morgan EF, Mason ZD, Chien KB, Pfeiffer AJ, Barnes GL, Einhorn TA, Gerstenfeld LC. 2009. Micro-computed tomography assessment of

fracture healing: relationships among callus structure, composition, and mechanical function. Bone. 44:335–344.
Murali K, Francis G, Madan R. 2011. Emerging Applications in Musculoskeletal CT Imaging. A GE Healthcare CT publication. 27–31.
Ouyang H. 1991. New discovery of upper Jurassic stegosaurian skin from Zigong, Sichuan. J Chengdu Coll Geol. 18:38–39. In Chinese.
Ouyang H, Pi XZ, Ye Y. 1998. A new discovery of sauropod skin fossil from Zigong, Sichuan. Jmineral Petrol. 18:146–149. In Chinese.
Peng GZ, Ye Y, Gao YH, Shu CK, Jiang S. 2005. Jurassic dinosaur faunas in Zigong. Chengdu: Sichuan people's publishing house; p. 1–236.
Qin Y. 2004. Fracture heeling, delayed union and nonunion. Chin J Orthop Trauma. 9:1059–1062.
Raven TJ, Maidment SCR. 2017. A new phylogeny of Stegosauria (Dinosauria, Ornithischia). Palaeontology. 60:401–408.
Rega E. 2012. Disease in dinosaurs. In: Brett-Surman MK, Holtz TRJ, Farlow JO, editors. The complete dinosaur. Bloomington (IN): Indiana University Press; p. 666–711.
Riminucci M, Fisher LW, Shenker A, Spiegel AM, Bianco P, Gehron RP. 1997. Fibrous dysplasia of bone in the McCune-Albright syndrome: abnormalities in bone formation. Amer J Pathol. 151:1587–1600.
Rothschild BM. 2010. Macroscopic recognition of nontraumatic osseous pathology in the postcranial skeletons of crocodilians and lizards. J Herpetol. 44:13–20.
Rothschild BM, Panza RK. 2005. Epidemiologic assessment of trauma-independent skeletal pathology in non-passerine birds from museum collections. Avian Pathol. 34:212–219.
Rothschild BM, Robinson L, Witt M, Koay J, Cline H. 2018. Radiologic/histologic discrepancies in tumor identification: the case of a "basketball-sized" mandibular tumor in a woman from 17th century West Virginia. Intl J Osteoarchaeol. doi:10.1002/oa.2.
Rothschild BM, Tanke DH. 2005. Theropod paleopathology: state of the art review. In: Carpenter K, editor. The canivorous dinosaurs. Bloomington (IN): Indiana University Press. 351–365.
Rothschild BM, Witzke BJ, Hershkovitz I. 1999. Metastatic cancer in the Jurassic. Lancet. 354:398.
Rothschild BM, Zheng XT, Martin L. 2012. Osteoarthritis in the early avian radiation: earliest recognition of the disease in birds. Cretaceous Res. 35:178–180.
Sampson SD, Witmer LM. 2007. Craniofacial anatomy of *Majungasaurus crenatissimus* (Theropoda: Abelisauridae) from the Late Cretaceous of Madagascar. J Vert Paleont. 27:32–102.
Straight WH, Davis GL, Skinner CW, Haims A, McClennan BL, Tanke DH. 2009. Bone lesions in hadrosaurs: computed tomographic imaging as a guide for paleohistologic and stable-isotope analysis. J Vert Paleontol. 29:315–325.
Sutton MD. 2008. Tomographic techniques for the study of exceptionally preserved fossils. Proc Bioll Sci. 275:1587–1593.
Wang J, Ye Y, Pei R, Tian Y, Feng CQ, Zheng DR, Chang SC. 2018. Age of Jurassic basal sauropods in Sichuan, China: a reappraisal of basal sauropod evolution. Geol Soc Am Bull. 130:1493–1500.
Witmer LM, Ridgely RC. 2008a. Structure of the brain cavity and inner ear of the centrosaurine ceratopsids dinosaur *Pachyrhinosaurus* based on CT scanning and 3D visualization. In: Currie PJ, Lanston W Jr., Tanke D, editors. A new horned dinosaur from an Upper Cretaceous bone bed in Alberta. Ottawa: NRC Research Press; p. 117–149.
Witmer LM, Ridgely RC. 2008b. The paranasal air sinuses of predatory and armored dinosaurs (Archosauria: Theropoda and Ankylosauria) and their contribution to cephalic structure. Anat Rec. 291:1362–1388.
Witzmann F, Asbach P, Remes K, Hampe O, Hilger A, Paulke A. 2008. Vertebral pathology in an ornithopod dinosaur: a hemivertebra in *Dysalotosaurus lettowvorbecki* from the Jurassic of Tanzania. Anat Rec. 291:1149–1155.
Witzmann F, Schwarz-Wings D, Hampe O, Fritsch G, Asbach P. 2014. Evidence of spondyloarthropathy in the spine of a phytosaur (Reptilia: Archosauriformes) from the Late Triassic of Halberstadt, Germany. PLoS One. 9:e85511.
Xing LD, Dong H, Peng GZ, Shu CK, Hu XD, Jiang H. 2009. A scapular fracture in *Yangchuanosaurus hepingensis* (Dinosauria: Theropoda). Geol Bull China. 28:1390–1395.
Xing LD, Rothschild BM, Randolph-Quinney PS, Wang Y, Parkinson AH, Ran H. 2018. Possible bite-induced abscess and osteomyelitis in *Lufengosaurus* (Dinosauria: Sauropodomorph) from the Lower Jurassic of the Yimen Basin, China. Sci Rep. 8:5045.
Zhou SW 1984. The Middle Jurassic dinosaurian fauna from Dashanpu, Zigong, Sichuan (Stegosaurs). Sichuan science and technology publishing house. 1–52.